Title
HEAVY-ION ELASTIC SCATTERING AT HIGH ENERGIES

Authors
Wang, W.L.
Lipes, R.G.

Publication Date
1973-08-01

Submitted to Phys. Rev.

LBL-1988
Preprint c.2

HEAVY-ION ELASTIC SCATTERING AT HIGH ENERGIES

W L. Wang and R. G. Lipes

August 1973

Prepared for the U. S. Atomic Energy Commission
under Contract W-7405-ENG-48

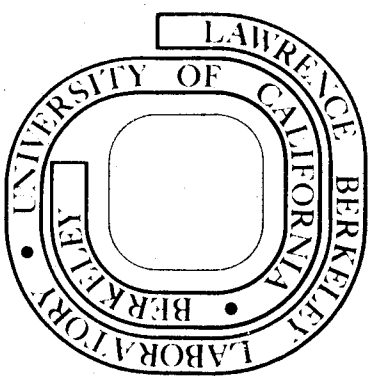

DISCLAIMER

HEAVY-ION ELASTIC SCATTERING AT HIGH ENERGIES*

W. L. Wang†

Carnegie-Mellon University
Pittsburgh, Pennsylvania 15213
and
Lawrence Berkeley Laboratory
University of California
Berkeley, California 94720

and

R. G. Lipes††

Carnegie-Mellon University
Pittsburgh, Pennsylvania 15213

August 1973

ABSTRACT

We investigate relativistic heavy-ion scattering in terms of a coherent droplet model, where the colliding nuclei are treated as droplets of nuclear matter with no internal structure. The interaction between nuclei is assumed to be proportional to the amount of interpenetrating matter. We take the matter distribution from electron scattering experiments, and relate the interaction parameter by optical theorem to the total cross section.

We have performed calculations at incident kinetic energies at 2.1 GeV/nucleon for ^{4}He, ^{12}C, and ^{16}O, and obtain a general diffraction pattern in the differential cross section. We also show some interesting scaling property among heavy-ion scattering, as compared to particle-nucleus or black-sphere scattering.

I. INTRODUCTION

There are some interesting speculations on the interaction of hadron matter at relativistic energies, such as the energies now available at Bevatron up to 2.1 GeV/nucleon.[1] Due to the large coherent aggregation of nucleons in the colliding nuclei, a state of enormous energy density may be obtained, where many species of hadrons and mesons may coexist. Aside from this speculation, the properties of nucleus-nucleus scattering are of interest in many fields, such as cosmic ray physics, particle physics and also nuclear physics.

In cosmic ray measurement, the secondary beam resulting from collisions of the primary cosmic ray with atmospheric nuclei must be separated out in order to study the composition of the primary cosmic ray. Such correction to the data requires a detail knowledge of the interaction length and fragmentation of nucleus-nucleus collision.

In terms of "nuclear democracy",[2] a nucleus with A nucleons is just an elementary particle with baryon number A. It is therefore interesting to study the particle physics aspect of nucleus-nucleus interaction. If the asymptotic region is attained, then a test of general concepts, such as limiting fragmentation, facterization, and diffractive dissociation should be possible. However, these reaction phenomenons usually require change of many degrees of freedom of the system; their detailed treatments are quite complicated.

In this report, we shall study a simple aspect of heavy-ion collision, i.e., the elastic scattering, which involves minimal change of degree of freedom. In keeping with the "nuclear democracy", our main interest is to see whether the nucleus-nucleus elastic scattering could be interpreted as simple hadron, e.g., proton-proton and pion-proton, collisions. It is well known that high energy elastic scattering at small angles generally depends only on the

matter distributions of the colliding objects. For nucleus-nucleus collision, the diffraction peak in the differential cross section, as we shall see, is surprisingly independent of the detail of the matter distribution. To demonstrate this point further, we compare our results to the extreme case of a sharp cut-off model, where interaction takes place only within a cut-off impact parameter. We also predict a scaling property in heavy-ion differential cross sections, which is compared to proton-proton and proton-nucleus scattering measurements.

II. BASIC FORMULATION

High-energy hadron elastic scattering from the nucleus has been quite successfully interpreted in terms of the multiple-diffraction theory of Glauber.[3] Recently the Glauber theory has been generalized by Czyż and Maximon[4] to the case of composite-particle scattering at high energies. They have obtained a complete multiple scattering series in terms of elementary scattering amplitudes between the basic constituents and the densities of the composite particles. Such a series may be reduced to a simple form in the optical limit when the numbers of constitutents (A and B) are large and the elementary scattering cross section σ is bound as $\sigma \sim (A \times B)^{-1}$. Czyż and Maximon[4] have also presented some model studies of the sensitivity of the diffraction pattern to the input parameters, both in multiple-scattering calculation and in the optical limit.

In this note, we would, however, like to take a slightly different point of view concerning nucleus-nucleus scattering at very high energies, although the formulation itself is equivalent to the optical limit of the Glauber theory. We think that it is useful, at such energies, to disregard the internal structure or

constitutents of the nucleus and take the nucleus to be a distribution of nuclear matter. The collision of two nuclei could then be discussed on the same footing as proton-proton scatterning, where no quarks or partons are necessary in the interpretation of their elastic scattering.

This coherent droplet model was first proposed by Chou and Yang[5] in their discussion of elementary particle scattering. Durand and Lipes[6] have applied the model to proton-proton elastic scattering and have shown a diffraction pattern which has recently been verified by experiments at CERN.[7] With this success, it is therefore of particular interest to study this model further in nucleus-nucleus high energy elastic scattering which may shed some light in the similarity in the hadron and nuclear interactions.

Following the coherent droplet model, we assume that 1) the elastic scattering is primarily diffractive, resulting from the absorption of the incident wave into inelastic channels, and 2) the absorption is proportional, for any impact parameter, to the total amount of interpenetrating nuclear matter. From assumption 2), we have th S-matrix at impact parameter b as

$$S(\vec{b}) = \exp\left[ix\int d^2b'\ \rho_A(\vec{b}')\rho_B(\vec{b}-\vec{b}')\right] \qquad (1)$$

where x is a possibly energy-dependent proportionality constant and $\rho(\vec{b})$ are the two-dimensional densities (or the blackness of the objects).[5] In analogy with the absorption of a wave propagating through a medium, we may write the complete elastic scattering amplitude as

$$F(\vec{q}) = \frac{ik}{2\pi}\int d^2b\ \exp[i\vec{q}\cdot\vec{b}]\left\{1 - S(\vec{b})\right\} \qquad (2)$$

where $\vec{q}$ is the momentum transfer, k is the incident momentum, and $q^2 = 2k^2(1-\cos\theta)$. We note that, in the optical limit of the Glauber thoery,

we have an identical expression, Eq. (2), for the scattering amplitude. In the case of the Glauber theory, the parameter x is complex and related to the nucleon-nucleon scattering amplitudes.[4] In our calculation, x is simply taken to be a constant to be determined by the total cross section.

Equation (2) is a convenient starting point for calculations using impact-parameter formalism. As an alternative, we would like to use angular momentum representation (or the partial wave expansion). To carry out the transformation, we first define the form factor $G(\vec{q})$ as two dimensional Fourier transform of the density

$$\rho(\vec{b}) = \int \frac{d^2\vec{q}}{(2\pi)^2} e^{-i\vec{q}\cdot\vec{b}} G(\vec{q}) \quad . \tag{3}$$

We may then integrate over $\vec{b}'$ in Eq. (1) and obtain

$$S(\vec{b}) = \exp\left[ix\int \frac{d^2\vec{q}}{(2\pi)^2} e^{-i\vec{q}\cdot\vec{b}} G_A(\vec{q})G_B(\vec{q})\right] . \tag{4}$$

If we further assume that the density is spherically (or conically) symmetric, then $G(\vec{q})$ is independent of the direction of $\vec{q}$. This allows us to integrate the exponent in Eq. (4) over the direction of $\vec{q}$; we have

$$S(b) = \exp\left[ix\int \frac{qdq}{(2\pi)} J_o(qb)\, G_A(q)G_B(q)\right] \quad , \tag{5}$$

which is independent of the direction of $\vec{b}$. The function $J_o(qb)$ is the zeroth order Bessel function. We may convert Eq. (5) into a partial wave scattering amplitude by introducing the following correspondence: $(kb \leftrightarrow \ell + \frac{1}{2})$. We therefore have $P_\ell(\cos\theta) \approx J_o(qb)$ for θ small and large ℓ,

$$\sum_\ell (2\ell+1) \sim \int_o^\infty 2k^2 bdb \tag{6}$$

and the partial wave amplitude $S(b) \rightarrow S_\ell(k)$ as

$$S_\ell(k) = \exp\left[ix\left(\frac{k^2}{2\pi}\right)\int d(\cos\theta) P_\ell(\cos\theta) G_A(q) G_B(q)\right] \quad . \tag{7}$$

Finally we may write the complete scattering amplitude $F(q)$ as

$$F(q) = \frac{1}{2ik} \sum_\ell (2\ell + 1) \left\{\exp[ixB_\ell(k)] - 1\right\} P_\ell(\cos\theta) \tag{8}$$

where θ is the center of mass angle, ℓ is the orbital angular momentum. The phase shift $\delta_\ell(k)$ is related to the projection of product form factor, or the phase shift function $B_\ell(k)$, by $2\delta_\ell(k) = ixB_\ell(k)$. Here $B_\ell(k)$ is given by

$$B_\ell(k) = \left(\frac{k^2}{2\pi}\right)\int_{-1}^{1} d(\cos\theta) P_\ell(\cos\theta)\, G_A(q)\, G_B(q) \quad , \tag{9}$$

which is identical to the following expansion

$$G_A(q)\, G_B(q) = \left(\frac{2\pi}{k^2}\right)\sum_\ell (2\ell+1)\, B_\ell(k)\, P_\ell(\cos\theta) \quad . \tag{10}$$

We may interpret $G_A(q)G_B(q)$ as the probability that the colliding heavy ions could sustain a momentum transfer q without being broken-up. It is also interesting to note that Eq. (8) is formally identical to the case of a single-particle scattering from a composite system, where $B_\ell(k)$ would be the partial wave amplitude associated with the form factor of the target alone.

We have now completed our basic formulation. For the differential cross section, we find it useful to introduce the invariant parameter $t = -q^2$ and the invariant differential cross section as

$$\frac{d\sigma}{dt} = \frac{\pi}{k^2} \left|F(q)\right|^2 \quad . \tag{11}$$

For reference, the c.m. angular distribution is $d\sigma/d\Omega = k^2(d\sigma/dt)$. The advantage of using the invariant cross section is that, in the asymptotic region where the parameter x is a constant, it becomes independent of incident energy. This can be best seen from Eq. (2) where $F(q) \propto k$ if S(b) is independent of energy.

The total cross section is given by the optical theorem as

$$\sigma_{tot}(k) = \frac{4\pi}{k} \text{Im}[F(q=0)] \ . \tag{12}$$

For simplification, we first take the parameter x to be purely imaginary: $x = ix_o$, where x_o is real and can be determined from a total cross section measurement. Explicitly we have

$$\sigma_{tot}(k) = \frac{2\pi}{k^2} \sum_{\ell} (2\ell+1) \left\{1 - \exp[-x_o B_\ell(k)]\right\} \tag{13}$$

In the asymptotic energy region, the total section may be taken to be simply the geometric value:

$$\sigma_{tot} = 2\pi(R_A+R_B)^2 \tag{14}$$

where R_A and R_B are the radii of the colliding nuclei. This choice of the channel radius is probably consistant with the assumption that the nucleus would break up whenever there is any appreciable amount of overlap of the nuclear matter. This range of interaction is also consistant with low-energy optical model calculation for heavy-ion elastic scattering.[8]

We may generalize the above discussion to allow the parameter x_o to be complex. Let us replace $x = (\beta+i)x_o$ in Eq. (1). Equation (8) for the scattering amplitude is unchanged. However, the total cross section now does not uniquely

specify our parameter. We have

$$\sigma_{tot} = \frac{2\pi}{k^2} \sum_{\ell} (2\ell+1) \left\{ 1 - \exp[-x_o B_\ell(k)] \cos(\beta x_o B_\ell) \right\} \qquad (15)$$

where we need an estimate of x_o or β. We first note that both the differential and total cross sections are independent of the sign of β. Furthermore, the parameter β would generally affect the differential cross section only near diffraction minima, but does not give rise to substantial change in the diffraction pattern, as shown by Czyż and Maximon[4] and also by Durand and Lipes.[6] In our calculation, we therefore set a value of β and use Eqs. (14) and (15) to determine x_o. As we shall show, the diffraction pattern presists even for β to be as large as 0.5. More interestingly, we could determine the sign of β from experiment by nuclear-Coulomb interference at small angles, which can then be compared with the real part of free nucleon-nucleon forward amplitude. This may give some insight to the degree of transparency in nucleus-nucleus scattering, as compared to nucleon-nucleon scattering.

III. MODEL CALCULATION

We would now like to apply the formulation to scattering of heavy ions. Since there are beams only of light nuclei available to test this model, we would like to restrict ourselves only to these nuclei. Generally we may represent their density distribution by Gaussian or a simple modified Gaussian form. In this case the numerical calculation simplifies greatly by allowing analytic expressions for $B_\ell(k)$ in Eq. (8). For other nuclei where a Woods-Saxon density distribution may be more appropriate, the impact parameter formalism may be simpler.

Let us use the following modified Gaussian form factor[9]

$$G_i(q) = [1 - \frac{\alpha_i}{2(2+3\alpha_i)} a_{m,i}^2 q^2] \exp[- a_{c,i}^2 q^2/4] \tag{16}$$

where i = A or B, $\alpha_i = (A_i-4)/6$ with A_i as the number of nucleons in the nucleus i. The parameters a_m and a_c are determined from electron scattering. To simplify the notations, let us introduce

$$a_i = \frac{\alpha_i}{2(2+3\alpha_i)} \; a_{m,i}^2 \tag{17}$$

$$b_i = a_{c,i}^2/4 \quad . \tag{18}$$

From Eq. (10), we obtain the following expression for $B_\ell(k)$:

$$\left(\frac{2\pi}{k^2}\right) B_\ell(k) = \exp[-u] \left\{[1-v+w+ \frac{\ell(v-2w)}{u} + \frac{w\ell(\ell-1)}{u^2}] \; i_\ell(u) + [v-2w+ \frac{(2\ell+1)w}{u}] \; i_{\ell+1}(u) + w i_{\ell+2}(u)\right\} ; \tag{19}$$

where we have defined

$$u = 2(b_A+b_B)k^2 \tag{20}$$

$$v = 2(a_B+a_B)k^2 \tag{21}$$

and

$$w = 4a_A a_B k^4 \quad . \tag{22}$$

The functions $i_\ell(u)$ are the modified spherical Bessel functions of the first kind.[10] The nuclear r.m.s. radius R_i is related to α_i and $a_{m,i}$ by

$$R_i = \sqrt{\frac{3(2+5\alpha_i)}{2(2+3\alpha_i)}} \; a_{m,i} \tag{23}$$

It might be useful to point out that the partial form factor $B_\ell(k)$ in Eq. (19), which has been extracted directly from Eq. (10), could also be obtained by using

$$B_\ell(k) = \sum_{\ell''\ell'} \begin{pmatrix} \ell'' & \ell' & \ell \\ 0 & 0 & 0 \end{pmatrix}^2 f^A_{\ell''}(k) f^B_{\ell'}(k) \left(\frac{k^2}{2\pi}\right) \tag{24}$$

where the round bracket indicates a Wigner 3-j symbol,[11] and the functions $f_\ell(k)$ are the partial form factors associated with the individual nucleus, i.e.,

$$G_A(q) = \sum_\ell (2\ell+1)\, f^A_\ell(k)\, P_\ell(\cos\theta) \quad . \tag{25}$$

We note again that our formulas are applicable to particle-nucleus scattering, if one of the form factors is properly chosen. In the Glauber theory, the projectile form factor will be related to nucleon-nucleon elastic scattering amplitude.

Before we discuss our results, we would like to recall the diffraction pattern of a black-sphere scattering.[12] That is, if we take

$$\begin{aligned} S(b) &= 0 \qquad b \leq R_1+R_2 \\ &= 1 \qquad b > R_1+R_2 \quad , \end{aligned} \tag{26}$$

the ratio of the differential cross sections is given simply by

$$\left(\frac{d\sigma}{dt}\right) \Big/ \left(\frac{d\sigma}{dt}\right)_{t=0} = 4\left|\frac{J_1(qR)}{qR}\right|^2 \tag{27}$$

where $J_1(qR)$ is the first order Bessel function. The factor 4 is due to the fact that $\lim_{x\to 0} J(x)/x = \frac{1}{2}$. The effective radius is $R = R_1 + R_2$. Equation (27) displays the well-known Fraunhofer diffraction. The cross section is sharply peaked in the forward direction, with minima occuring at the zeros of $J_1(qR)$. We shall see that,

in the case of nucleus-nucleus and particle-nucleus collisions, this diffraction pattern is very rapidly attained, especially when the nucleus has a relatively sharp surface region. In the next section, we shall discuss the results of our calculation and compare them to particle-nucleus and the black-sphere scattering. In our calculations, we do not take into account the Coulomb scattering, which is important only at very small angles at such high energies for light nuclei.

IV. NUMERICAL RESULTS

In this section we shall discuss some general features of heavy-ion scattering. For our examples we would like to restrict ourselves to the light nuclei, such as ^{4}He, ^{12}C, and ^{16}O. Their density distributions have been well studied by electron scattering.[9] The parameters for the form factors, as represented by Eq. (16), are given in Table I. We are first interested in the behavior of the partial wave form factors $f_\ell(k)$ in Eq. (25) and the phase shift function $B_\ell(k)$ in Eq. (10) or (19); two such examples are given in Fig. 1, where we notice that the $B_\ell(k)$ and $f_\ell(k)$ do fall rapidly after a transient region of angular momentum, which would be sensitive to the nuclear surface. However, as we shall see, the smooth fall off in Fig. 1 results in quite similar differential cross section to a sharp cut-off model. This is probably due to a very large number of partial waves contributing to the differential cross section calculations, so that the transient region is relatively narrow.

With the phase shift functions $B_\ell(k)$, we may obtain the scattering amplitude $F(q)$ in Eq. (8), provided that the parameter x is determined from Eq. (13) or (15). The values of the parameter x, the total cross section $\sigma_{(tot)}(k)$ and total elastic cross section $\sigma_{el}(k)$ are given in Table II, where we also show the ratio σ_{el}/σ_{tot}. We note that not only the magnitudes of the total elastic cross section depends on the value of x, but also the diffraction pattern. In Fig. 2, we show the dependence of the total and elastic cross sections, and the position of the first minimum in the differential cross section as functions of the parameter x. The ratio σ_{el}/σ_{tot} approaches 0.5 for very large x_o, which indicates strong absorption probability (see Eq. (1)). For different value of x, the differential cross section is very different as shown by Czyż and Maximon[4] in their study of the

composite particle scattering. (Here we refer to their study of the effects of the subunit size which they renormalize. Their parameter ABσ is related to x in our model.) In Fig. 2, it is also interesting to see that the position of the first minimum, let us call it t_{min}, is not determined by the size of the colliding objects alone, It is clear that σ_{tot}, σ_{el} and t_{min} are all inter-dependent through the parameter x. However, if σ_{tot} or σ_{el} is determined by the size of the colliding objects, the position t_{min} may then depend on the size alone.

We may now calculate the differential cross sectons, which are shown in Fig. 3. The solid lines indicate the purely diffractive scattering (β=0); the dashed lines show the results with a large value of β. Other intermediate values of β, e.g. $\beta = 0.2$, would give slightly more pronounced minima than those shown by the dashed line. Our purpose is to show that, even for such large β, the diffraction pattern still remain, except at very large momentum transfer. The maxima are not, however, affected by the value of β. We note again that the diffraction patterns shown in Fig. 5 are independent of the incident energy (see the discussion following Eq. (11)).

In Table III, we show some quantities of interest related to the differential cross section $(\frac{d\sigma}{d\Omega})_{c.m.}$ similar to Fig. 3. This is useful for comparison to other experimental results generally shown in terms of the non-invariant form $(d\sigma/d\Omega)_{c.m.}$. It is interesting to note that the values of the product qR at the minima for all the reactions remain constant and rather close to the black-sphere values (see the discussion following Eq. (27)). This feature is particularly interesting if we recall that the $B_\ell(k)$ in Fig. 1 do not seem to have a very sharp cutoff in ℓ. Nevertheless, a cutoff is shown in Fig. 1 may be deemed "sharp" as far as producing the minima is concerned.

We now compare the region of mementum transfer near the first diffraction minimum of heavy-ion scattering to those of particle-nucleus and proton-proton scattering in Fig. 4. These three types of scattering cover a very large range of mementum transfer. The large size of heavy ions emphasizes the importance of the very small momentum transfer region.

We have now shown the general behavior of the differential cross section in heavy-ion scattering. The most interesting feature of our study is the regularity of the diffraction minima, expressed in terms of the values of qR, as shown in Table III. To illustrate this property further, we plot the relative cross section $(d\sigma/dt)/(d\sigma/dt)_{t=0}$ versus qR in Fig. 5. It is quite interesting that the cross sections seem to scale, especially within the first minimum. We notice that the cross section of ^{16}O-^{16}O is nearly equal to that of ^{12}C-^{12}C scattering at all momentum transfer. This seems to be a limiting case for heavy-ion scattering. In Fig. 5, we also compare our results to black-sphere scattering. Although the minima are predicted by the black-sphere model, the magnitude is generally too large at large momentum transfer. There is more large-angle scattering in the black-sphere model, due to the sharp surface. For a nucleus with more diffused surface, such as ^{4}He-^{4}He case, the large-angle scattering is relatively smaller. It is also interesting, at this point, to point out some similarities between the particle-nucleus and the nucleus-nucleus scattering. We note from the high energy data of p-^{4}He, p-^{12}C and p-^{16}O experiments[13] that diffraction minima also occur quite close to the values given by the sharp cut-off model. The relative differential cross section, as plotted in Fig. 5, at the second maximum seems to have an asymptotic value of 0.2×10^{-2}. The large-angle scattering in particle-nucleus scattering becomes much smaller than that in nucleus-nucleus scattering; this is consistent with our observation that proton has a much more diffused surface. These particle-nucleus scattering have been discussed by several authors in the framework of the Glauber theory.[4,14]

Finally we would like to demonstrate one more property of the model. If we increase or decrease the radius of ^{4}He, the total cross section (therefore the absorption parameter x) and the total elastic scatterings cross section will all be changed, but the plot in the coordinates qR of Fig. 5 will not be very much changed. We show such an effect in Fig. 6, where we have increased or decreased the radius by about 10%. The diffraction pattern remains the same. This property would also appear in the optical limit calculation of the Glauber theory as applied to particle-nucleus scattering at high energies. It is worthwhile to note that the form factors are quite different in the momentum transfer region involved in the calculation, as shown in the inset of Fig. 6. It is important to see that this specific feature will not occur if we just make the nuclear matter denser or looser as is done in Ref. 4, in which case the parameter x (or $AB\sigma$) is not changed; we, however, have changed x to give the new total cross section as specified by Eq. (14).

V. CONCLUDING REMARKS

We have investigated the general behavior of heavy-ion scattering at relativistic energies. In this asymptotic region, we have shown that there is a scaling property in the differential cross section. It is appropriate to reiterate the purpose of this study: We are interested in the elementary-particle aspect of nucleus-nucleus collisions. We postulate that the elastic scattering is determined by the matter distributions of the colliding nuclei, and that scattering phenomenon can be treated on the same footing as proton-proton or pion-proton scattering. The degrees of freedom of the "subunits" in the nucleus can be completely neglected. The nucleus-nucleus scattering is directly related to electron scattering through the use of the form factors. In this model, the total cross section and the complete differential cross section are directly interrelated through the absorption parameter; this is more general than the optical theorem where the total cross section is related only to the imaginary part of the forward scattering amplitude.

To test this model, we suggest the following experiments: 1) scattering of nuclei with very diffused surface, e.g. deutron or helium, to study the large momentum transfer, and 2) scattering of nuclei heavier than ^{12}C to study the asymptotic behavior of the diffraction pattern. Nuclei heavier than ^{16}O would generally have a similar, or sharper, diffuseness on the surface and, therefore, should give similar diffraction pattern. It would also be interesting to use beams of various energies to determine the energy where the interaction becomes asymptotic. There is evidence from fragmentation experiments that the asymptotic region is reached at as low as 1 GeV/nucleon.[15]

In our formalism, we have not made use of the assumption of pre-existing subunits, such as nucleons. This model should be valid since we are dealing with elastic scattering where no internal degrees of freedom are disturbed. A microscopic treatment, such as the Glauber theory, is certainly more useful if nucleonic correlation effects are important and can be properly taken into account. In this case, the nuclear structure information may be extracted from such experiments. It would be particularly interesting if the effects of nucleonic correlations become enhanced in heavy-ion scattering due to some coherent collision processes, which are not present in particle-nucleus scattering. This possibility should be investigated when such data are available in the near future.

We would also like to mention that a similar approach has been applied to low-energy heavy-ion elastic scattering.[16]

FOOTNOTES AND REFERENCES

* Work performed under the auspices of the U. S. Atomic Energy Commission, and supported in part by the National Science Foundation.

† Present address: University of California, Lawrence Berkeley Laboratory, Berkeley, California 94720.

†† Present address: California Institute of Technology, Pasadena, California 91109.

1. H. A. Grunder, W. O. Hartsough, and E. J. Lofgren, Science 174, 1128 (1971); M. G. White, M. Isaila, K. Prelec, and H. L. Allen, Science 174, 1121 (1971); H. H. Heckman, D. E. Greiner, P. J. Lindstrom, and F. S. Bieser, Phys. Rev. Letters 28, 926 (1972).

2. See for example, M. Jacob and G. F. Chew, Strong Interaction Physics (W. A. Benjamin, Inc., New York, 1964).

3. R. J. Glauber in, Lectures in Theoretical Physics, Vol. I (Interscience Publ. Inc., New York 1959); R. J. Glauber in, High Energy Physics and Nuclear Structure, ed. by G. Alexander, North-Holland Pub. Co, Amsterdam (1967).

4. W. Czyż and L. C. Maximon, Ann. Phys. 52, 59 (1969).

5. T. T. Chou and C. N. Yang, Phys. Rev. Letters 20, 1213 (1968); Phys. Rev. 170, 1591 (1968); Phys. Rev. 175, 1832 (1968).

6. L. Durand and R. Lipes, Phys. Rev. Letters 20, 637 (1968).

7. C. Rubbia, report in the XVI International Conference on High-Energy Physisc, Batavia (1972).

8. For reference, see Proceedings of Heavy-Ion Summer Study (June 12-July 1, 1972), Oak Ridge National Laboratory, Oak Ridge, Tennessee. Report # CONF-720669, ed. S. T. Thornton.

9. R. Hofstadter, Ann. Rev. Nucl. Sci. 7, 231 (1957); H. F. Ehrenberg, R. Hofstadter, U. Meyer-Berkhout, D. G. Ravenhall, and S. E. Sobottka, Phys. Rev. 113, 666 (1959); I. Sick and J. McCarthy, Nucl. Phys. A150, 631 (1970).

10. M. Abramowitz and I. S. Stegun, Handbook of Mathematical Functions (Dover Pub. Inc., New York 1965).

11. A. R. Edmonds, Angular Momentum in Quantum Mechanics (Princeton Univ. Press, Princeton, 1957).

12. H. A. Bethe and G. Placzek, Phys. Rev. 51, 450 (1937).

13. H. Palevsky, J. L. Friedes, R. J. Sutter, G. W. Bennett, G. J. Igo, W. D. Simpson, G. C. Phillips, D. M. Corley, N. S. Wall, R. L. Stearns, and B. Gottschalk, Phys. Rev. Letters 18, 1200 (1967).

14. R. Bassel and C. Wilkin, Phys. Rev. Letters 18, 871 (1967); Czyż and L. Lesniak, Phys. Letters 24B, 227 (1967); J. Formánek and J. S. Trefil, Nucl. Phys. B3, 155 (1967); J. P. Auger and R. J. Lombard, Phys. Letters 45B, 115 (1973).

15. D. E. Greiner, private communications.

16. C. B. Dover and J. P. Vary, Bull. Am. Phys. Soc. II 18, 601 (1973); B. Fink and C. Toepffer, Phys. Letters 45B, 411 (1973).

Table I. Parameters for Nuclear Form Factors

Nucleus	a_m (fm)	a_c (fm)	α	$\sqrt{\langle r^2 \rangle}$ (fm)
^{4}He	1.31[a]	1.31	0.0	1.61
^{12}C	1.66	1.59	$\frac{4}{3}$	2.45
^{16}O	1.76	1.70	2	2.64

[a]Note that this value is used to calculate the r.m.s. radius only; the parameter α=0 in Eq. (16), in the case of ^{4}He.

Table II. Absorption Parameters and the Corresponding Total and Total Elastic Cross Sections[a]

	x_o	σ_{tot} (mb) the geometric value)	σ_{el} (mb)	$\frac{\sigma_{el}}{\sigma_{tot}}$
$^4He - ^4He$	5.6×10^3	630	241	0.382
$^4He - ^{12}C$	1.0×10^4	1030	407	0.394
$^4He - O^{16}$	1.1×10^4	1130	445	0.394
$^{12}C - ^{12}C$	1.7×10^4	1500	605	0.403
$^{12}C - ^{16}O$	1.8×10^4	1620	655	0.404
$^{16}O - ^{16}O$	1.9×10^4	1750	706	0.403

[a]For $\beta = 0.2$.

Table III. Some Quantities of Interest in the Differential Cross Sections.[a]

Reactions	Differential Cross Section at $\theta = 0$ $\frac{d\sigma}{d\Omega}$ ($\frac{barn}{sr}$)	Position of 1st Minimum		Differential Cross Section at 2nd Maximum $\frac{d\sigma}{d\Omega}$ ($\frac{barn}{sr}$)	Position of 2nd Minimum		Differential Cross Section at 3rd Maximum $\frac{d\sigma}{d\Omega}$ ($\frac{barn}{sr}$)	Incident Momentum in C.M. System ($\frac{GeV}{c}$)
		qR	θ_{cm}(degree)		qR	θ_{cm}(degree)		
$^4He - ^4He$	3.08×10^2	3.9	4.6	1.7	7.4	8.7	0.07	3.9
$^4He - ^{12}C$	2.15×10^3	3.9	2.13	15.1	7.2	3.9	0.8	6.35
$^4He - ^{16}O$	3.18×10^3	3.9	1.84	21.7	7.2	3.4	1.1	6.99
$^{12}C - ^{12}C$	1.55×10^4	3.9	0.95	121.8	7.1	1.7	7.8	11.56
$^{12}C - ^{16}O$	2.38×10^4	3.9	0.78	158.8	7.1	1.4	12.1	13.28
$^{16}O - ^{16}O$	3.71×10^4	3.9	0.65	296.1	7.1	1.2	18.6	15.4
Black-Sphere Scattering		3.8			7.1			

[a]For $\beta = 0.2$.

FIGURE CAPTIONS

Fig. 1. Partial wave expansion of nuclear form factors $f_\ell(k)$ and the phase shift functions $B_\ell(k)$ as defined by Eqs. (10) and (25). The dashed line is $f_\ell(u)$ and the solid line is $B_\ell(k)$. The form factor $f_\ell(u)$ is essentially the phase shift function in particle-nucleus scattering. These functions are constant at small ℓ and vanish after transition near the value $\ell = kR$.

Fig. 2. The total cross section and the total elastic cross section as a function of the absorption parameter x_o. For this illustration we take $\beta = 0$. For very large x_o, the ratio σ_{el}/σ_{tot} approaches 0.5 as given by a black-sphere scattering. The position of the first minimum t_{min} also depends on the parameter x_o.

Fig. 3. Differential cross sections for ^4He-^4He, ^4He-^{12}C and ^{12}C-^{12}C elastic scattering. The solid line is obtained using a purely imaginary x, i.e., $x = ix_o$; the dashed line corresponds to $x = (\beta+i)x_o$, with a large real part $\beta = 0.5$. The real part does not affect the diffraction pattern very much, except at the minima or large momentum transfer. The diffraction patterns shown here are independent of the incident energy.

Fig. 4. Comparison of heavy-ion scattering with other types of scattering. The regions of interest are the diffraction patterns within the second maximum. Heavy-ion scattering covers a very different momentum transfer region. The proton-proton scattering is from Ref. 6 and 7; the p-^4He and p-^{16}O calculations in the optical limit are from Ref. 4. The p-p scattering data drops by a factor of 10^{-7} at the second maximum; the smaller momentum transfer region is not reproduced here. Note that the cross sections are in arbitrary unit.

Fig. 5. Differential cross sections in "scaling coordinates". We plot relative cross section, $(d\sigma/dt)$ to the forward cross section $(d\sigma/dt)_{t=0}$, versus qR, where q is the momentum transfer and R is the effective radius $R = R_1 + R_2$. The differential cross sections seem to scale. The ^{12}C-^{12}C, ^{12}C-^{16}O, and ^{16}O-^{16}O are essentially indistinguishable on this plot. The ^4He scattering diviates from the symptotic form, probably due to its diffused surface. The long dashed line is the prediction of a sharp cut-off model (black-sphere scattering).

Fig. 6. Test of sensitivity of the "scaling plot" to changes of nuclear radius for ^4He-^4He scattering. The form factors are shown in the upper right inset. It is clear that although the angular distribution are different, the "scaling plots" remain nearly identical.

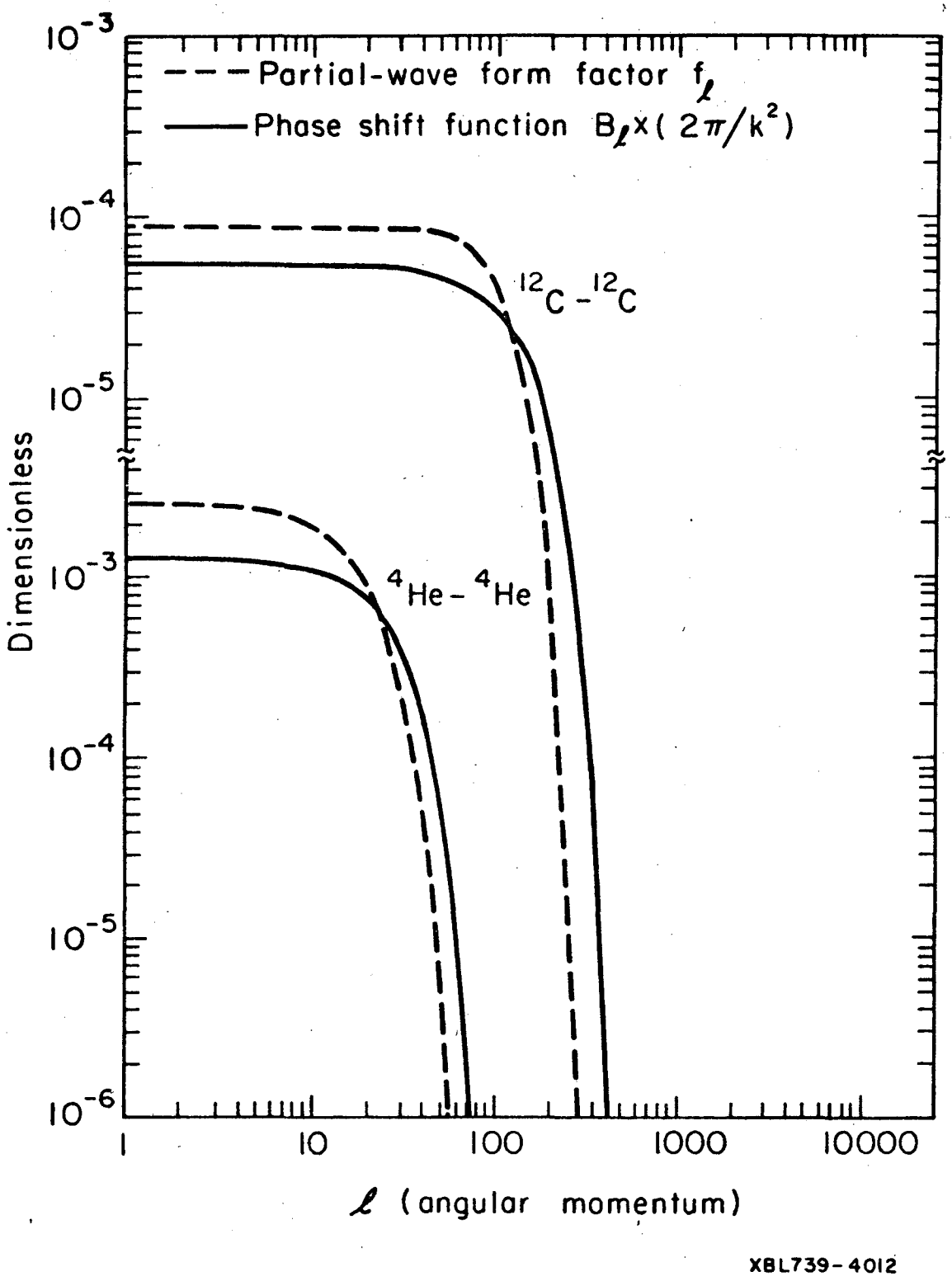
Partial-wave form factor f_ℓ
Phase shift function $B_\ell \times (2\pi/k^2)$
$^{12}C - ^{12}C$
$^{4}He - ^{4}He$
Dimensionless
10^{-3}
10^{-4}
10^{-5}
10^{-3}
10^{-4}
10^{-5}
10^{-6}
1
10
100
1000
10000
ℓ (angular momentum)
XBL739-4012

Fig. 1

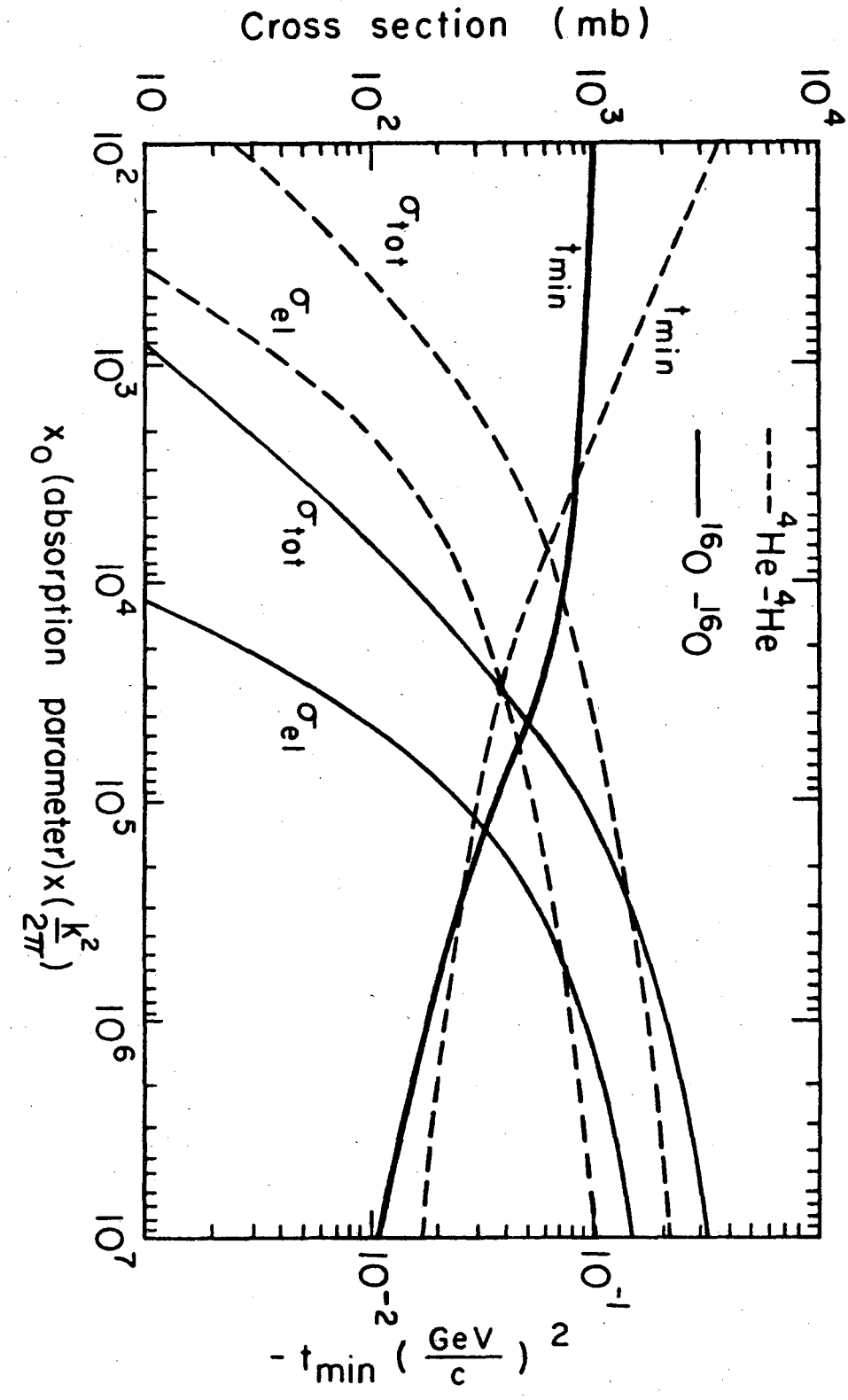
Cross section (mb)
10
10^2
10^3
10^4
10^2
10^3
10^4
10^5
10^6
10^7
σ_{tot}
σ_{el}
t_{min}
t_{min}
σ_{tot}
σ_{el}
^{16}O - ^{16}O
^4He - ^4He
x_0 (absorption parameter) $\times (\frac{k^2}{2\pi})$
10^{-2}
10^{-1}
$-t_{min} (\frac{GeV}{c})^2$
XBL739-4013

Fig. 2

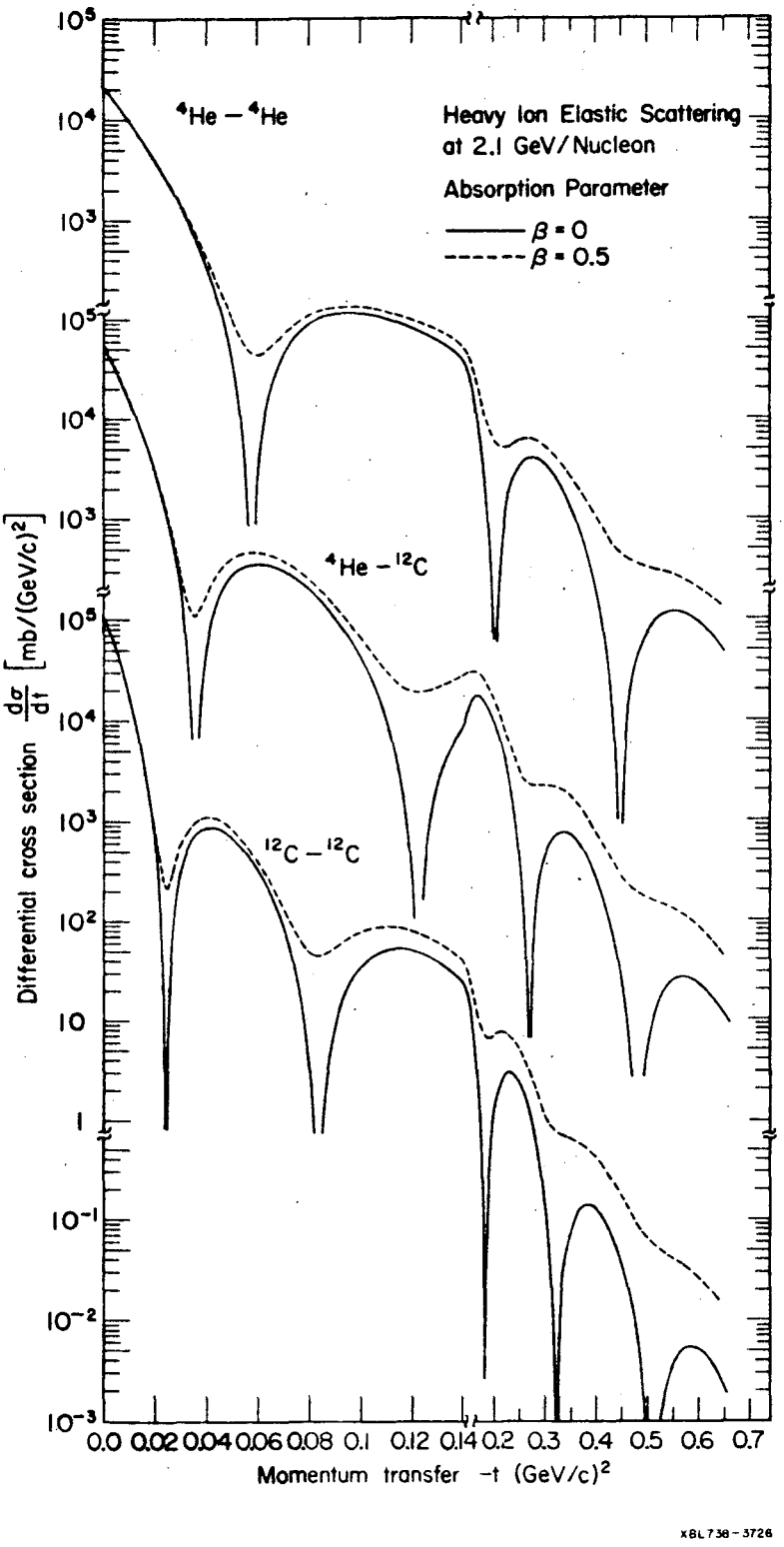
Heavy Ion Elastic Scattering
at 2.1 GeV/Nucleon
Absorption Parameter
β = 0
β = 0.5
⁴He – ⁴He
⁴He – ¹²C
¹²C – ¹²C
Differential cross section dσ/dt [mb/(GeV/c)²]
Momentum transfer –t (GeV/c)²
0.0 0.02 0.04 0.06 0.08 0.1 0.12 0.14 0.2 0.3 0.4 0.5 0.6 0.7
XBL738-3726

Fig. 3

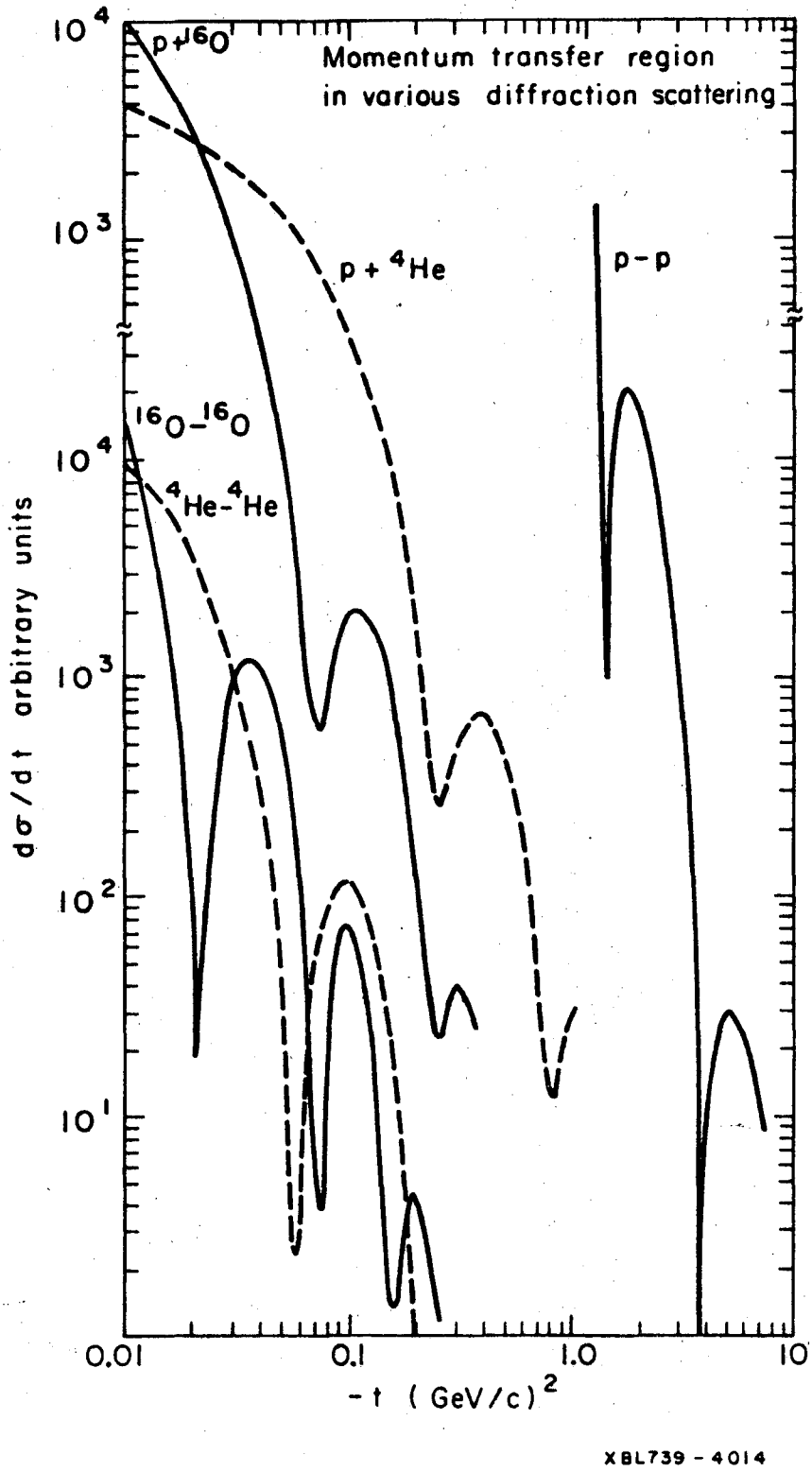
Momentum transfer region
in various diffraction scattering
p+16O
p + 4He
p-p
16O-16O
4He-4He
dσ/dt arbitrary units
-t (GeV/c)2
0.01
0.1
1.0
10
XBL739-4014

Fig. 4

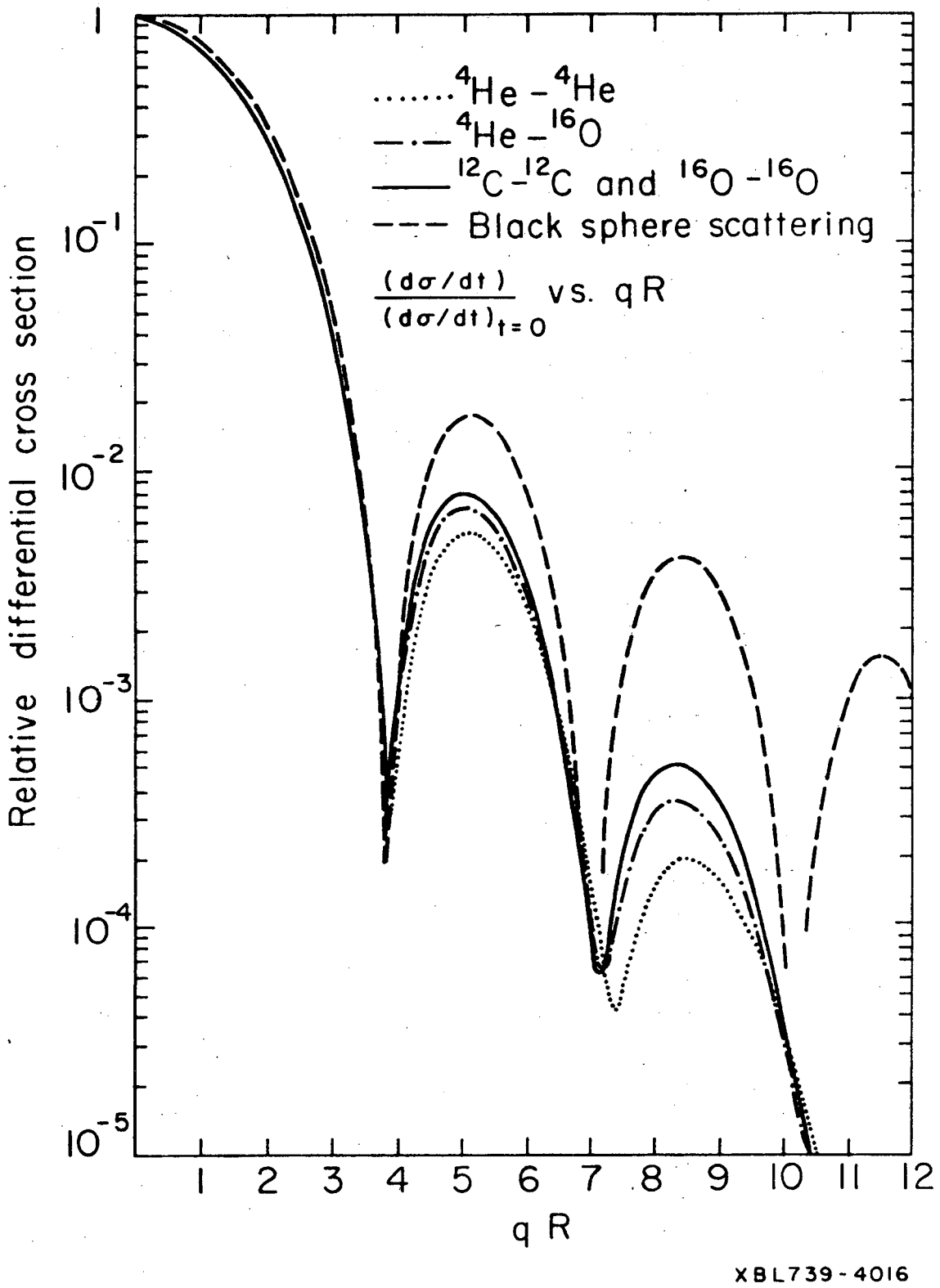
Relative differential cross section
1
10^{-1}
10^{-2}
10^{-3}
10^{-4}
10^{-5}
1 2 3 4 5 6 7 8 9 10 11 12
q R
$^4He - ^4He$
$^4He - ^{16}O$
$^{12}C - ^{12}C$ and $^{16}O - ^{16}O$
Black sphere scattering
$\frac{(d\sigma/dt)}{(d\sigma/dt)_{t=0}}$ vs. qR
XBL739-4016

Fig. 5

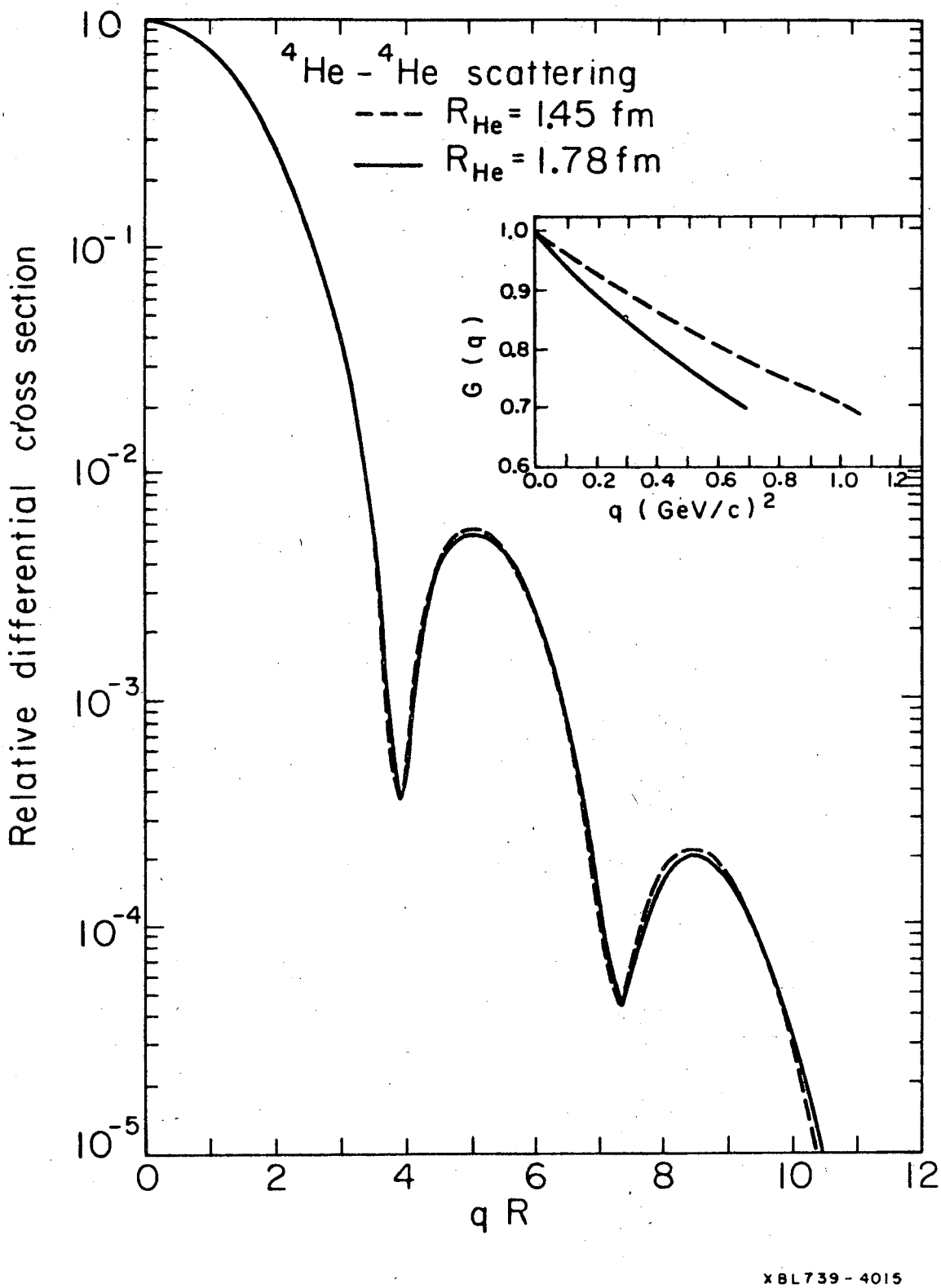
^{4}He - ^{4}He scattering
--- R_{He} = 1.45 fm
—— R_{He} = 1.78 fm
Relative differential cross section
10
10^{-1}
10^{-2}
10^{-3}
10^{-4}
10^{-5}
0
2
4
6
8
10
12
q R
G (q)
1.0
0.9
0.8
0.7
0.6
0.0
0.2
0.4
0.6
0.8
1.0
1.2
q (GeV/c)^2
XBL739-4015

Fig. 6

TECHNICAL INFORMATION DIVISION
LAWRENCE BERKELEY LABORATORY
UNIVERSITY OF CALIFORNIA
BERKELEY, CALIFORNIA 94720